Journal of Applied Ecology | BRITISH ECOLOGICAL SOCIETY

RESEARCH ARTICLE

Clustered and rotating designs as a strategy to obtain precise detection rates in camera trapping studies

Pablo Palencia[1,2,3] | **Jorge Sereno-Cadierno**[2] | **Davide Carniato**[2] | **Tiago Marques**[4,5] | **Tim R. Hofmeester**[6] | **Joaquin Vicente**[2] | **Pelayo Acevedo**[2]

[1]Department of Biology of Organisms and Systems, University of Oviedo, Biodiversity Research Institute (University of Oviedo-CSIC-Principado de Asturias), Mieres, Spain; [2]Institute for Game and Wildlife Research (IREC) CSIC-UCLM-JCCM, Ciudad Real, Spain; [3]Department of Veterinary Sciences, Largo Paolo Braccini, University of Turin, Torino, Italy; [4]Centre for Research into Ecological and Environmental Modelling (CREEM), University of St Andrews, St Andrews, UK; [5]Departamento de Biologia Animal, Centro de Estatística e Aplicações, Faculdade de Ciências da Universidade de Lisboa, Lisbon, Portugal and [6]Department of Wildlife, Fish, and Environmental Studies, Swedish University of Agricultural Sciences, Umeå, Sweden

Correspondence
Pablo Palencia
Email: palenciapablo@uniovi.es and palencia.pablo.m@gmail.com

Abstract

1. Camera traps have transformed the way we monitor wildlife and are now routinely used to address questions from a wide range of ecological and conservation aspects. Sampling design optimization and a better understanding of drivers determining the precision of detection rates (i.e. the number of detections per unit of effort) are important methodological issues. Little attention has been focused on the effect of placing more than one camera on each sampling point (hereafter, clustered design), and/or rotating (i.e. redeploying) the cameras to new placements during the sampling period.

2. We explored the differences in the precision of detection rates between clustered vs. single camera designs when cameras remained in the same location during the study. Furthermore, the effect of keeping the placement of cameras fixed or rotating them (i.e. moving them to new locations during the sampling period), when a limited number of camera devices are available, was also evaluated. We used simulations and field data to test differences in detection rate precision for the different sampling designs. We simulated three different population distributions (random, trail-based and aggregated) and three abundance scenarios. The simulations were validated with a field experiment focused on eight species with different behavioural traits, including artiodactyls, carnivores, lagomorphs, and birds.

3. When a fixed number of sampling points were monitored simultaneously, clustered designs generally resulted in an increase in the precision of detection rates compared to single designs. The absolute reduction in the coefficient of variation by clustered designs was on average 0.07 units (min: 0.01, max: 0.15), which represents an average relative reduction in CV of 31% (min:6%, max:44%). An improvement in precision was also observed as a higher number of sampling points

was used for all population distributions and sampling designs tested. When a fixed number of cameras were available, rotating the cameras to independent locations improved precision (an absolute reduction of 0.19 CV units) when monitoring aggregated populations, but not for random and trail-based population distributions.

4. *Synthesis and applications*: Our research provides a guideline for wildlife managers and researchers to improve the precision of camera trap detection rates and optimize resource allocation. In general, the study design should accommodate the behaviour of the target species (e.g. spatial aggregation and abundance), monitoring program logistic resources (both human and economic) and study area characteristics (e.g. accessibility and vandalism).

KEYWORDS
abundance, camera traps, ecology, encounter rate, imperfect detection, sampling design, trapping rate, wildlife

1 | INTRODUCTION

Camera traps are used around the world by scientists to study wildlife populations in a wide range of habitats and latitudes. Constant progress in technology, falling prices over time (Agha et al., 2018), and advances in data management software (Forrester et al., 2016; Scotson et al., 2017; Vélez et al., 2022) have enabled the spread of their use in wildlife management and conservation. Camera traps are now used to address questions from a wide range of ecological, management, and conservation aspects (Delisle et al., 2021; ENETWILD-consortium et al., 2023).

The detection of an individual by a camera trap is determined by a plethora of factors (Hofmeester et al., 2019). The detection process has been generally referred to as the combination of the ecological (i.e. the site is occupied or not by the species) and observational processes (i.e. the species is detected or not given that it is present). Although the ecological process is out of the scope of human decisions, the observational process is not. Sampling design, including camera trap placement and settings, camera model and/or brand, survey length, number of placements, and use of lures and/or attractants, among others, determine the detection rate (i.e. the number of detections per unit of effort) in camera trapping studies (du Preez et al., 2014; Hofmeester et al., 2019; Kays et al., 2020, 2021; Palencia, Vicente, et al., 2022). Survey effort is typically measured as camera days (i.e. the number of camera traps used multiplied by the number of days they were in operation, Rovero & Zimmermann, 2016). The detection rate can be also referred to as the encounter rate, detection frequency, photographic rate or passage rate. Direct indices are frequently derived from detection rates as basic descriptors of species' presence—such as naïve occupancy (proportion of sampling points where a species has been observed)—and species' abundance—such as the relative abundance index, RAIs, (e.g. detection rate specified per 100 days; Carbone et al., 2001; Palmer et al., 2018;

Sollmann et al., 2013). However, detection rates do not account for imperfect detection (i.e. individuals/species present but not detected). Thus, the comparison of RAIs across time, species, space, or others is not reliable due to a variation in the detection rate that cannot be unambiguously attributed to actual differences in abundance but may have arisen from differences in detection (e.g. Anderson, 2001; Hofmeester et al., 2019). Similarly, naïve occupancy will result in underestimates of true occupancy due to false absences (i.e. species present but not detected, MacKenzie et al., 2002). More robust methodologies that account for imperfect detection when estimating occupancy and abundance have been described and are recommended. In general, the large variability in the detection rate among sampling points has been acknowledged, and usually, it determines most of the precision in the ecological parameter (e.g. population density, Howe et al., 2017; Palencia, Barroso, et al., 2022; Palencia et al., 2021). More precise detection rates will subsequently imply an improvement in precision in the ecological parameter.

Survey design has been a common research topic in camera trapping studies (Guillera-Arroita & Lahoz-Monfort, 2012; Hamel et al., 2013; Kays et al., 2020, 2021; Rich et al., 2019), both to optimize the detection process, improve the precision of the estimates and to better understand the drivers that determine the detection capability of the cameras (Jacobs & Ausband, 2018; Palencia, Vicente, et al., 2022). Designs based on targeted placements and the use of lures and attractants could be used to increase detection probability (du Preez et al., 2014; Stewart et al., 2019; Tourani et al., 2020); but random designs are mandatory to allow unbiased estimation for many analytical methods (e.g. Howe et al., 2017; Moeller et al., 2018; Nakashima et al., 2018; Rowcliffe et al., 2008). Additionally, both in targeted/lured and random designs, the most common practice is to place only one camera at each sampling point. The cost associated with the equipment usually limits the total number of cameras available to one per sampling point,

to eventually maximize the number of sampling points sampled and cover wider areas. Exceptionally, two cameras per sampling point are usually placed when individual identification of animals is needed (Green et al., 2020); but in these settings, cameras are placed facing each other to record pictures of both sides of the animals, and the microsite area surveyed overlaps.

The improvements in detectability due to the number of placements, survey duration and/or camera trap settings have been broadly explored (Kays et al., 2020; Palencia, Barroso, et al., 2022; Palencia, Vicente, et al., 2022), but little research has been conducted to assess the extent to which data collected at a single point are a consistent and repeatable measure of species presence and use of the habitat patch, and lastly, other ecological-related parameters (Hofmeester et al., 2021; Kays et al., 2021; Wong et al., 2019). Recent studies have evidenced the high variability in detection rate at small spatial scales (Evans et al., 2019; Hofmeester et al., 2021; Kolowski et al., 2021; Kolowski & Forrester, 2017). Across five focal species, Kolowski et al. (2021) evidenced a nearly total absence of spatial autocorrelation (i.e. data collected at one given site are independent to data collected at neighbouring sites) in detection rates at any distance, for any species in any season in a high-intensity grid with less than 20 m inter-camera spacing. Additionally, the authors found that local covariates that may influence detectability explained only a small proportion of the variation in the detection rates (Kolowski et al., 2021). A lack of spatial autocorrelation in cameras more than 25 m apart was also reported for mammals in a rainforest (Kays et al., 2010), and an empirical study in which camera traps were placed 10 m apart concluded that single cameras were not likely to represent the animal activity of the surrounding area for most of the species (Kays et al., 2021). All these results suggest a high level of unpredictability and randomness in the observation process, especially when attractants/bait are not used. While the high variation at smaller scales has been reported, little attention has been paid to the effect of placing multiple cameras at each sampling point to represent an average detection rate (hereafter clustered designs). Few studies have shown an improvement in occupancy and richness estimates when using clustered designs (Pease et al., 2016; Wong et al., 2019). Further research is needed to better understand sampling design strategies to improve the precision of estimates, especially concerning the potential reduction in the detection rate variance. In this respect, while its utility has been acknowledged (Kays et al., 2021), the effect of clustered designs on the precision of the detection rate has been overlooked.

From a practical point of view, clustered designs could become prohibitive due to the large number of camera devices needed. If a limited number of camera devices is available, a rotating approach (i.e. moving the camera location during the sampling period) could be a more flexible procedure to transition from a single design to a clustered one (ENETWILD-consortium et al., 2023). In this respect, a trade-off between the length of the monitoring period at sampling points and the number of sampling points emerges. The cost of the devices and the human effort needed to arrive at predetermined sampling points limit the number of camera traps and relocations to different sampling points in practice, respectively (Fuller et al., 2022; Si et al., 2014). However, it has not been investigated if rotating the cameras inside a cluster improves the precision of detection rate estimates compared to rotating the cameras to independent placements or not moving the cameras at all.

Considering all the above, the further investigation of sampling design decisions to obtain more precise detection rates will contribute to improving the precision and accuracy of the ecological parameter estimated (e.g. abundance or occupancy, Hofmeester et al., 2021; Howe et al., 2017; Kays et al., 2021; Palencia, Barroso, et al., 2022). Here, working in a simulation framework and an experimental field study, our objective was to assess the improvement in detection rate precision (i) when considering clustered designs given a fixed number of sampling points and (ii) when a given number of devices are available, comparing rotating cameras to new locations against keeping fixed camera placements. We hypothesized that clustered designs would provide a better representation of the presence and activity of the animals in the surrounding area of each sampling point and would thus increase the precision of detection rate estimates. Similarly, we expected that rotating the cameras to new placements (independent and/or clustered ones) would also increase the precision of detection rate estimates.

2 | MATERIALS AND METHODS

2.1 | Simulations

In a 2-dimensional space of 25 km^2 (5 × 5 km), we simulated three spatial point processes representing animal distribution, three different point intensities representing animal abundance scenarios, and two design strategies (static and rotating, see details below). In this simulation, each point represents a location visited by an animal.

2.1.1 | Spatial point process

We simulated random, trail-based, and aggregated spatial point processes representing animal distributions (Figure 1). In the random scenario, the points were randomly distributed through the study area. In the trail-based scenario, we first simulated a set of 75 random lines through the study area. Then, we distributed 20% of the points in 35 m buffers around those lines and the remaining 80% were randomly distributed throughout the study area. This distribution of points was based on the use of linear features reported for some mammals. For example, 16% of the GPS-collared Iberian lynx (*Lynx pardinus*) locations were found on trails and roads (Garrote et al., 2021), thus we used 20% as a reference value. For comparison purposes, we also simulated a trail-based scenario in which 50% of the points were distributed around the lines, and the remaining 50% were randomly distributed, see Appendix S1 in Supporting Information for further details. In the aggregated scenario, we
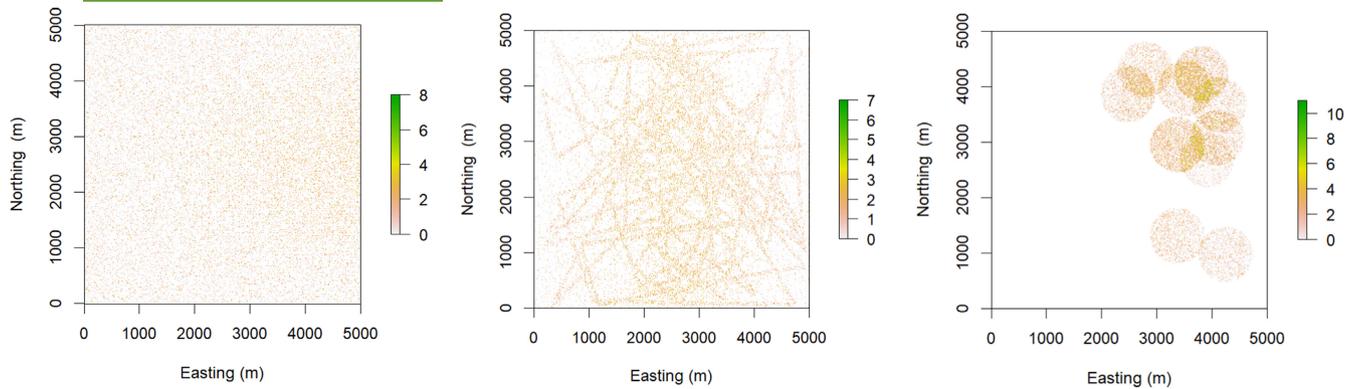
FIGURE 1 Examples of simulated spatial point patterns: random (left panel), trail-based (central panel), and aggregated (right panel). The study area is divided into 10×10 m squares and the scale indicates the number of points counted on each one.

simulated 10 circular buffers with a radius of 500 m, within which we used a Poisson process to generate aggregated points. The centres of the buffers were randomly distributed. Each scenario was replicated 1000 times. Finally, we also simulated three intensities for the point process (low, 90,000, medium; 180,000 and high: 360,000 points), representing increasing levels of abundance.

The points were then aggregated into 10×10 m squares. Thus, a square with a point count of 5 could represent 5 different individuals using this square, or a single individual using the square 5 times. This approximation represents the type of data recorded in camera trapping: for 5 records of a species at the same camera trap, we do not know, in general, whether they are 5 different individuals or the same individual recorded five times. This is always the case when individual recognition is not possible due to the absence of natural or artificial marks.

2.1.2 | Camera trap designs

We compared static and rotated designs. In the former, all the sampling points were monitored for the full duration of the survey period (cameras remained in the same location the entire period). In the latter, the cameras were rotated (moved) to new, either independent or clustered, placements during the survey period, resulting in each sampling point only being sampled during part of the survey period.

Fixed number of sampling points: Static approach
Regular grids (5×5, 6×6, 7×7, and 8×8) of sampling points (i.e. camera sites) were distributed covering the entire study area (Figure 2). A 10×10 m square (grid cell) was considered as the area sampled by a camera. Thus, all the point locations generated by the spatial process and that fell in a certain square represented the number of detections of that camera (i.e. perfect detection in the cell was assumed). In the single design, we placed one camera (i.e. 10×10 m grid cell) per sampling point. In the clustered design, we placed two additional cameras in a buffer of 50 m radius around the location where the first camera was located, resulting in three cameras (i.e. 3 grid cells) per sampling point in clustered designs, (Figure 2—upper

panels). The cameras remained in the same location throughout the survey period. Using this simulation we also compared clustered and single designs in terms of the number of cameras, and not only sampling points (i.e. 75 cameras deployed in a single design –75 sampling points-, or deployed in a clustered design –25 sampling points).

Fixed number of camera devices: Rotated approach
We also evaluated which rotation strategy resulted in the highest precision when a fixed number of devices were available (Figure 2—bottom panels). Specifically, we compared three regular grid designs under a scenario in which 15 cameras were available: (i) a 3×5 grid in which the cameras were fixed in the 15 initial locations (control scenario due to its cost-effectiveness), (ii) a rotating survey in which the 15 cameras were moved to new locations twice to finally monitor 45 independent sampling points (5×9 grid), and (iii) a rotating survey in which the 15 cameras were moved twice to new locations inside the 50 m buffer to finally monitor 45 locations clustered on 15 independent sampling points (3×5 grid). In the rotating approaches, we re-assigned the point count for each camera (square) considering that the survey effort of this design would be one third of the survey effort simulated. Specifically, we generated a number following a binomial distribution in which the size corresponds to the number of points counted in this square during the entire monitoring period, and the probability of success 1/3.

The R packages used to run the simulation were raster (Robert, 2023), dplyr (Wickham et al., 2023), sp (Pebesma & Bivand, 2005), data. table (Dowle & Srinivasan, 2021), rgeos (Bivand & Rundel, 2021) and spatstat.random (Baddeley & Turner, 2005). Simulations were coded in R (R Core Team, 2022), and the code to replicate the simulations can be found in Appendix S2.

2.2 | Field data experience

We sampled one natural area to evaluate the performance of clustered and rotated designs in field settings. The field experiment was carried out in Cabañeros National Park (39.3964 N, −4.4872 W, Central Spain, Figure 3). The administrative services
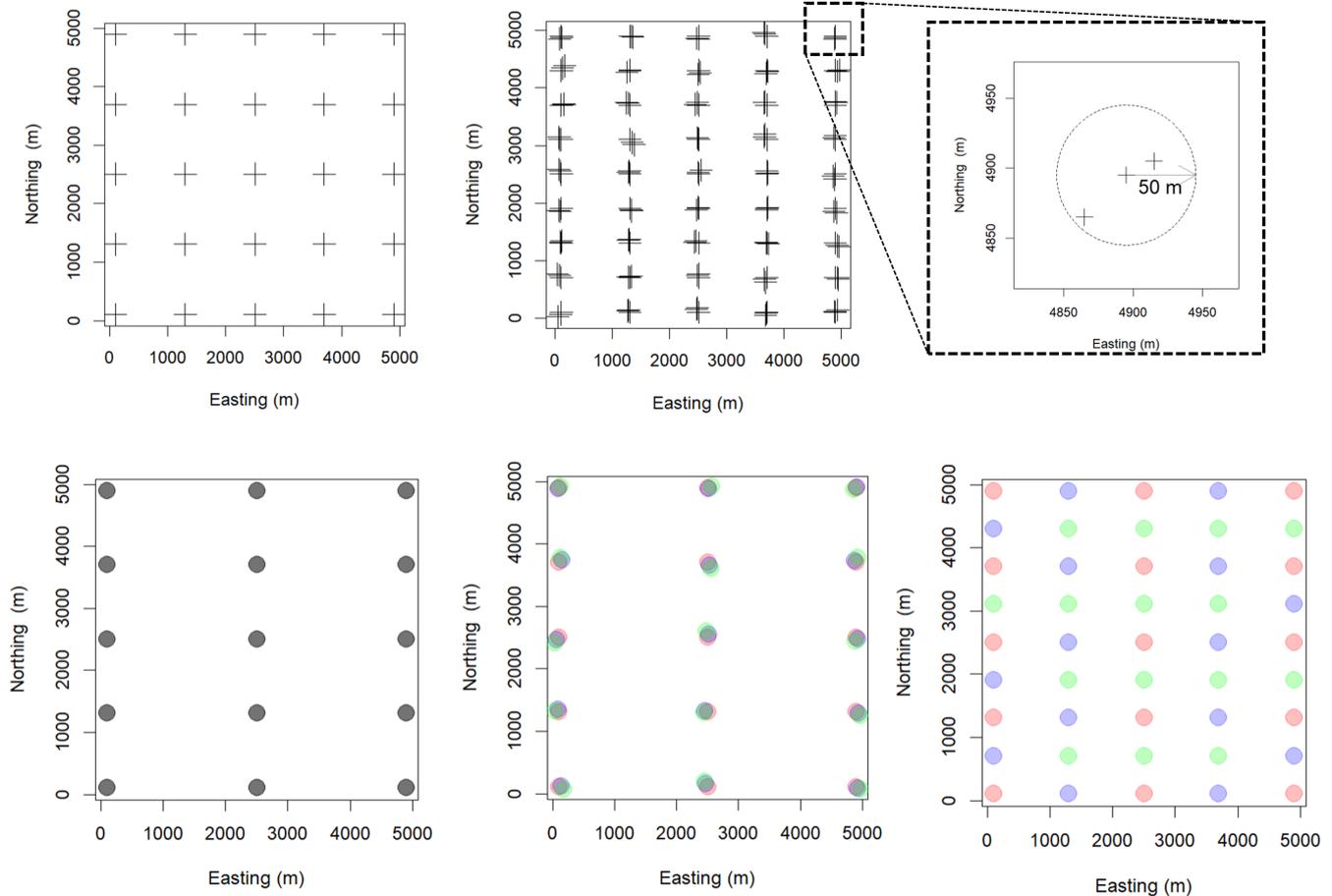
FIGURE 2 Single and clustered designs compared. The upper left panel represents a single design in which one camera trap (cross) is placed on each sampling point. The upper central panel represents a clustered design in which three camera traps (crosses) were placed in a buffer of a 50-m radius. The right-upper panel represents a zoom to one clustered sampling point in which three cameras are placed in a buffer of 50m radius. The bottom panels represent three different design strategies when 15 camera devices are available. The bottom left panel represents a design in which cameras are placed in a fixed location on the 3×5 single-regular grid for the entire survey period. The bottom-central penal represents a design in which cameras were rotated twice during the survey period but within a 50m buffer around the original locations on a 3×5 clustered regular grid; cameras were first placed on red points and subsequently moved to blue and green locations. The bottom-right panel represents a design in which cameras were rotated twice during the survey period to finally sample a 9×5 single-regular grid; cameras were first placed on red points and subsequently moved to blue and green locations. For interpretation of the references to colour in this figure legend, the reader is referred to the web version of this article.

of the National Parke authorized the experiment. The land is occupied mainly by three ecosystems: Iberian savannah-like habitats that are dominated by scattered *Quercus spp* trees (commonly known as "*dehesa*"), dense scrubland dominated by *Cistus* spp., *Salvia rosmarinus*, *Erica* spp., *Arbutus unedo*, and *Phyllirea angusti-folia*, and some patches covered by *Quercus faginea*, *Q. rotundifolia* and *Q. suber* forests. From 28 February to 5 May 2022, we deployed a camera trap grid in the ecotone between dense scrubland and dehesa with 60 sampling points 500m apart (Figure 3). Eighteen of these points were deployed following a clustered design containing three cameras per station in a 50m radius (Figure 3). StrikeForce and ReconForce Browning cameras were used (the same camera model was used in all clusters). Ethical approval was not required.

All cameras were placed 40cm above the ground and programmed to take images when activated by an animal in eight-shot groups. For the field data, independent detections were defined as images recorded more than 10min apart.

2.3 | Data analysis

To estimate the standard error of the detection rate, a non-parametric bootstrap (resampling sampling points with replacement) with 999 iterations was implemented (Buckland et al., 2001; Rowcliffe et al., 2008). The coefficient of variation (CV) was estimated by dividing the standard error of the detection rate by the mean detection rate. In clustered designs (both in static and rotated approaches), we first estimated the average mean of detections on each sampling point (i.e. arithmetic mean of the detection rate of the three cameras in a cluster), to finally estimate the CV as described above. We considered that a given design had a reasonable effect on precision when (i) it reduced
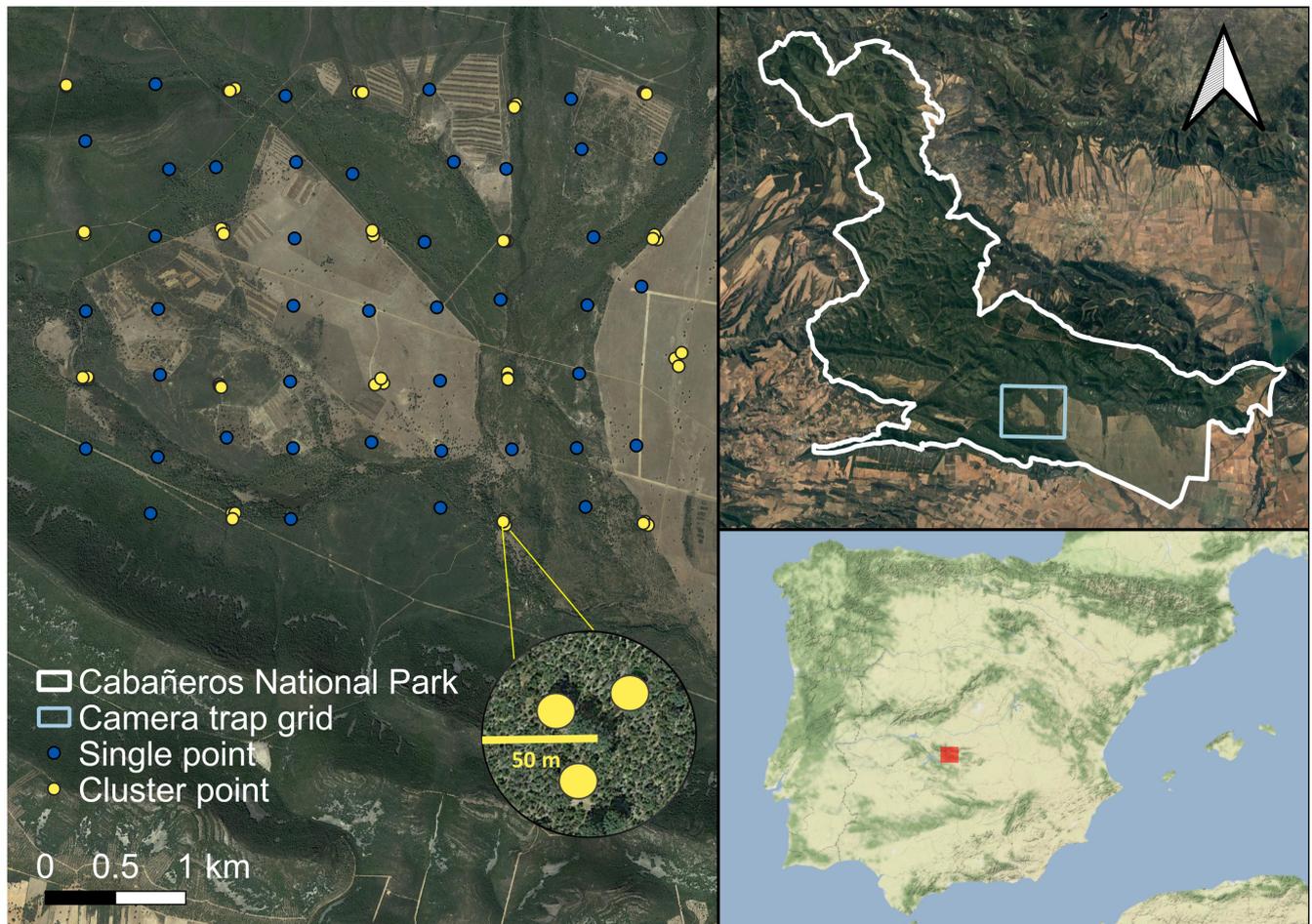
FIGURE 3 Fieldwork experiment carried out in Cabañeros National Park, Spain. Bottom-right panel: location of the study area (red square) in Spain. Upper-right panel: Cabañeros National Park boundaries (white line) and location of the monitored area (blue square). Left panel: location of the sampling points (camera traps). Blue represents single sampling point (i.e. one camera per sampling point), while yellow represents clustered sampling points (i.e. three cameras per sampling point in a 50 m radius plot). Background maps and orthophotos from Google Maps were used. For interpretation of the references to colour in this figure legend, the reader is referred to the web version of this article.

CV by 0.1 or more in absolute terms (e.g. CV reduced from 0.3 to 0.1); or (ii) it reduced CV by 20% or more in relative terms (e.g. CV reduced from 0.15 to 0.1, relative reduction of 33%). Thus, a reduction in absolute CV ≥0.1 or a relative reduction in CV ≥20% would support the use of this specific design to increase precision. In this analysis, we only considered those simulation replicates in which animals were detected at more than one sampling point.

2.3.1 | Specific considerations on field data

In addition to the analytical procedure described above, specific analyses were applied to field data to assess the population level of aggregation. First, for each species with a minimum of 20 detections (see Section 3), we assessed aggregation in counts by fitting Poisson or negative binomial distribution models to the detection rate (in the single designs) by using fitdistrplus R package (Delignette-Muller & Dutang, 2015).

Second, similarly to the static approach described above, we compared the CV obtained at the clustered sampling points, against the CV obtained at the same number of sampling points, but considering single cameras (Figure 3).

Third, to explore the effect of a rotated approach on the field data, we subsampled the detection rates in three different ways to recreate a scenario in which only 15 camera devices were used. Specifically, (i) we randomly selected 15 sampling points and considered the entire monitoring period (66 consecutive days); (ii) we randomly selected three groups of 15 sampling points and considered a monitoring period of 22 days for each one (thus, similarly to the simulation, created a dataset where cameras were rotated to a new position every 22 days); and (iii) from the 15 sampling points in which a clustered design was used, we randomly selected one camera of each cluster and considered a monitoring period of 22 days (thus, similarly to the simulation, created a dataset where cameras were rotated to a new position inside the cluster every 22 days; Figure 2).

3 | RESULTS

### 3.1 | Fixed number of sampling points: Static approach

3.1.1 | Simulations

When the same number of sampling points was monitored, the clustered design generally resulted in a slight increase in precision (i.e. lower coefficients of variation—CV) compared with single designs (Figure 4). On average, clustered designs reduced the CV by 0.08 under random animal distribution (relative reduction of 42.57%), by 0.09 under the trail-based animal distribution (relative reduction of 40.91%), and by 0.04 for aggregated animal distribution (relative reduction of 9.53%) (Appendix S3). We also observed that the difference in precision between clustered and single designs became smaller as underlying point intensity increased (considering the three distributions simulated, clustered designs reduced the CV by 0.10 -a 33.30% relative reduction- when 90,000 points were simulated, by 0.07 for 180,000 points -a 32.07% relative reduction-, and by 0.04 when 360,000 points were simulated -a 27.64% relative reduction-, Appendix S3). The naturally expected improvement in precision was also observed with a higher number of sampling points for all the point distributions and sampling designs (Figure 4). The average CV decreased from 0.35

(single) and 0.26 (clustered) when monitoring 25 sampling points, to 0.20 (single) and 0.15 (clustered) when monitoring 64 sampling points (Appendix S3). For random and trail-based distributions, similar values were obtained when a similar number of cameras were used, regardless if they were distributed in a single or cluster design. For example, the CV obtained in a clustered design with 25 sampling points (i.e. 75 cameras) was equivalent to a single design with 64 sampling points (i.e. 64 cameras; Figure 4). In contrast, for aggregated animal distributions, single-design deployments resulted in more precise detection rates in comparison to clustered designs (Appendix S3).

3.1.2 | Field data

We included those species in the analysis for which more than 20 independent encounters were recorded: red deer (*Cervus elaphus*), wild boar (*Sus scrofa*), roe deer (*Capreolus capreolus*), red fox (*Vulpes vulpes*), stone marten (*Martes foina*), badger (*Meles meles*), Iberian hare (*Lepus granatensis*), and red-legged partridge (*Alectoris rufa*). Three clustered sampling points were discarded due to camera failures. Therefore, we analysed 45 single sampling points (45×1), 15 clustered sampling points (15×3) to account for an equivalent number of camera devices, and 15 single sampling points (15×1) to account for an equivalent number of sampling points.
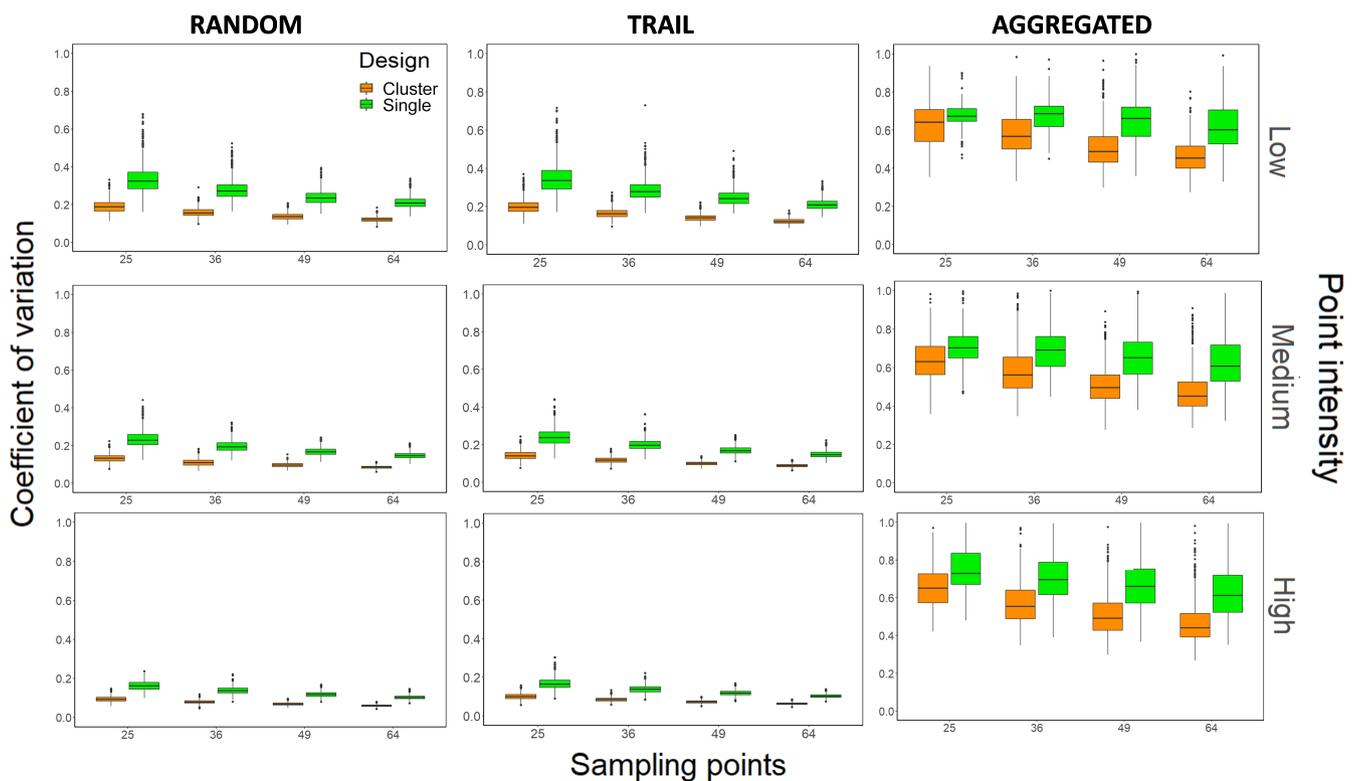
FIGURE 4 Precision results from the simulations. The coefficient of variation (*y*-axis) is plotted against the number of sampling points (*x*-axis) for the three distribution settings (random left panels, trail-based central panels and aggregated right panels), and the three-point intensity scenarios (90,000 points—upper panels, 180,000 points—central panels, and 360,000 points—bottom panels). While in single designs only one camera was placed at each sampling point, in the cluster ones, three cameras were placed in each sampling point. For interpretation of the references to colour in this figure legend, the reader is referred to the web version of this article.

When assessing population aggregation, the negative binomial distribution was supported against the Poisson distribution for the detection rates of all species, indicating a high level of aggregation in all the species (Figure 5). The estimated k overdispersion parameter ranged from 0.11 (badger) to 4.18 (wild boar) (the lower the k parameter, the higher the overdispersion; Bolker, 2008). The precision of the detection rate increased as the aggregation decreased for all species and sampling designs. The clustered design was generally more precise (CV = 0.33) than the single design (CV = 0.46) when monitoring 15 sampling points. When comparing 45 cameras distributed in a single design (45 × 1, Figure 5), or aggregated into a clustered design (i.e. 15 × 3, Figure 5), the former returns a slightly lower

(ca. 0.05 lower) CV, especially when the aggregation was not very high (i.e. k overdispersion parameter was higher than 0.5, Figure 5).

3.2 | Fixed number of camera devices: Rotated approach

3.2.1 | Simulations

All these results refer to simulations in which 15 cameras (devices) were available. When aggregated distributions were simulated, keeping the camera trap locations fixed or rotating the cameras inside the
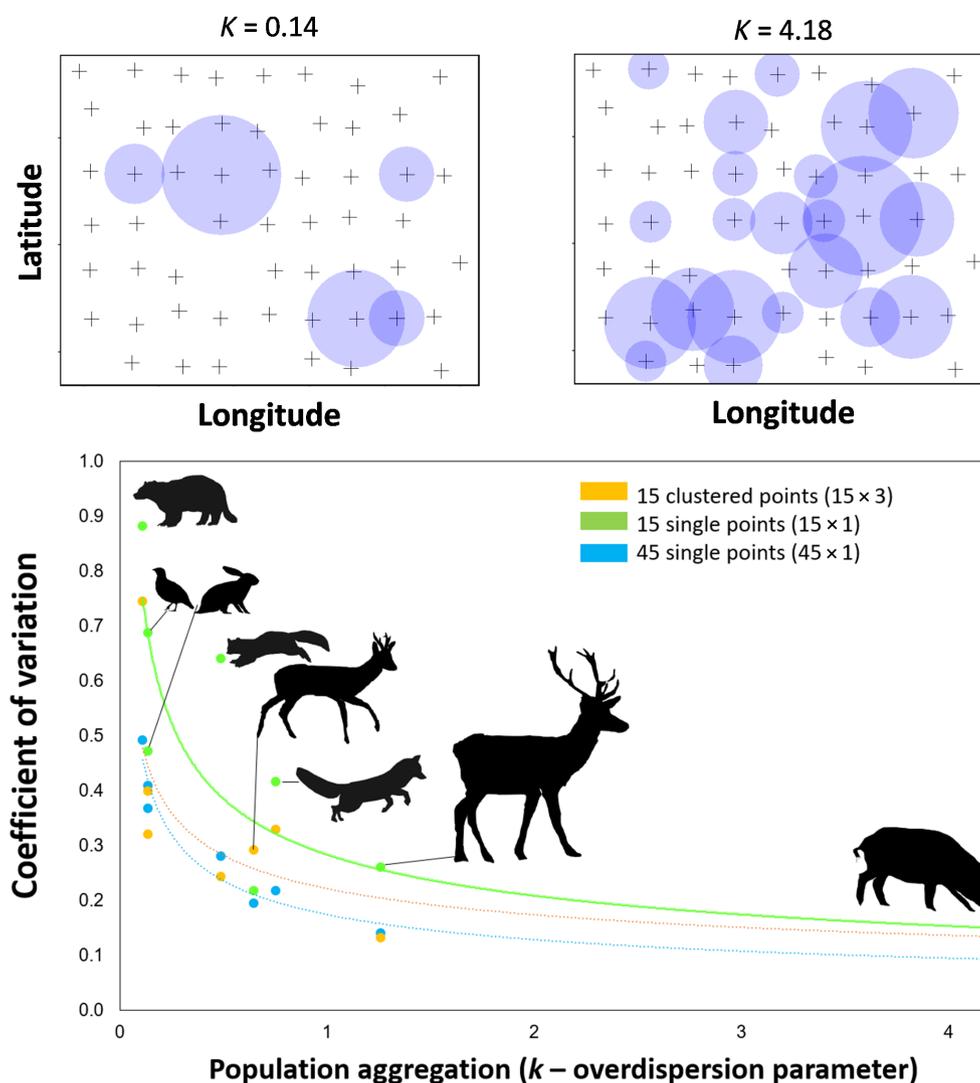
FIGURE 5 Relation between population aggregation and precision in real populations. The upper panels show two scenarios of population aggregation, from highly aggregated (top left, partridge, k = 0.14) to less aggregated (top right, wild boar, k = 4.18). In the upper panels, the size of the circle is proportional to the number of encounters at the trap on the centre of the circle. The lower panel represents the increase in precision (lower coefficient of variation) in relation to a decrease in population aggregation (higher k-values). The K-value is the overdispersion parameter of a negative binomial distribution and measured the degree of aggregation in the data (here, the aggregation on the encounter histories of the 45 cameras), the lower the k, the higher the overdispersion. The lines represent a potential fit to the data (CV = $a \cdot k^b$). Silhouettes represent the target species from the most aggregated (left) to the least aggregated (right): badger, red-legged partridge, Iberian hare, stone marten, roe deer, red fox, red deer, and wild boar. For interpretation of the references to colour in this figure legend, the reader is referred to the web version of this article.
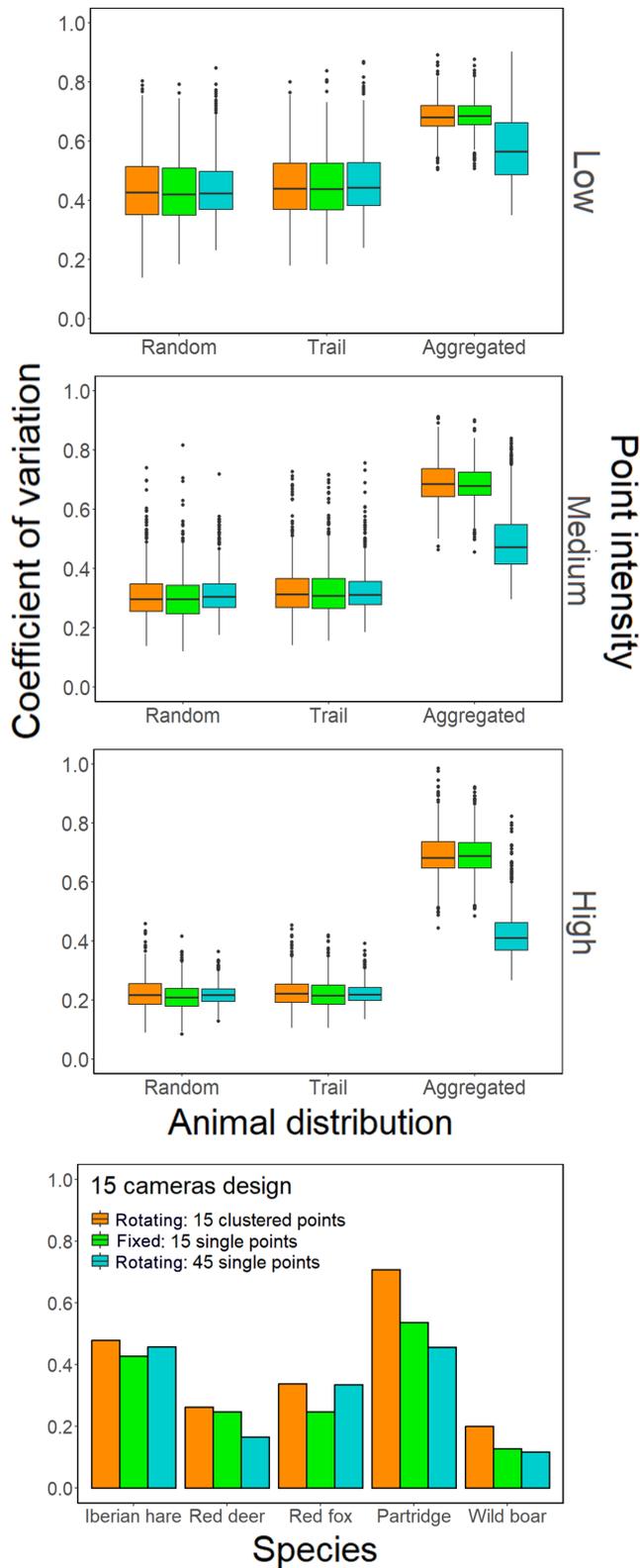
FIGURE 6 Precision obtained when using 15 camera traps, where the total amount of effort is the same in all designs. Orange represents a design in which the 15 cameras were moved to new locations within the cluster during the sampling period to finally sample a 3×5 clustered regular grid. Green represents a design in which the 15 cameras are kept fixed in the same position during the entire sampling period to finally sample a 3×5 single-regular grid. Blue represents a design in which the 15 cameras were moved to new independent locations during the sampling period to finally sample a 5×9 single-regular grid. The three upper panels represent simulation results under three scenarios of point intensity, from the lower (upper panel) to the higher (bottom panel). Results obtained in the field study are shown in the bottom panel, including the Iberian hare (*Lepus granatensis*), red deer (*Cervus elaphus*), red fox (*Vulpes vulpes*), partridge (*Alectoris rufa*) and wild boar (*Sus scrofa*). For interpretation of the references to colour in this figure legend, the reader is referred to the web version of this article.

similar CVs (Figure 6). For instance, with low-point intensity and random point distribution, the CV obtained was 0.43 when the cameras were kept in the same location, and 0.44 when they were rotated inside the cluster or to independent placements (Figure 6, Appendix S3).

3.2.2 | Field data

Regarding the field data, rotating the cameras to independent placements resulted in the lowest CV (on average, 0.30), while rotating inside the cluster resulted in a CV of 0.40, and keeping the cameras fixed resulted in a CV of 0.32 (Figure 6). Rotating the cameras to independent locations returned the lowest CV in red deer, red partridge, and wild boar (Figure 6). Alternatively, keeping the location of the cameras fixed during the entire survey period returned the lowest CV for the Iberian hare and red fox (Figure 6).

4 | DISCUSSION

Working in a simulated framework and with field data, we illustrated that clustered designs slightly improve precision in camera trap detection rates when a constant number of sampling points are monitored simultaneously (cameras remained in the same location the entire survey period) regardless of how animals are distributed over a study area (Figures 4 and 5). When a limited number of camera devices is available, rotating (moving) cameras to independent placements could be desirable to increase precision for spatially aggregated populations because we found a reduction of 0.2 units in CV with this design (Figure 6).

Previous studies have described the absence of spatial autocorrelation in capture rates even at small (10–100m) distances (Kays et al., 2010; Kolowski et al., 2021), and it has been recommended to place multiple cameras at each sampling point to obtain an average value for the habitat patch and minimize bias associated with single locations (Hofmeester et al., 2021; Kays et al., 2021). Our study corroborates these recommendations, both for simulated and empirical data. We found high variability in detection rates

cluster resulted in an average CV of 0.69 in both cases. However, we observed an increase in precision when rotating cameras to independent placements (Figure 6); we obtained an average CV of 0.50 (i.e. a reduction of 0.19 in CV, Appendix S3). For trail-based and random point distributions, maintaining the location of the cameras, rotating them in the cluster, or rotating them to independent locations resulted in

among the clustered cameras (i.e. cameras placed close together, a 50 m radius buffer in this study, Figure 1). The intra-cluster variability corroborates the convenience of clustered designs to better represent the species' use of the sampling point and surroundings. On the other hand, the inter-cluster variability in detection rates was still high, thus the improvement in precision was relatively low (lower than 0.1 units in CV for all the spatial point patterns simulated, Figure 4). More than three cameras per sampling point will increase the precision -and the difference between single and cluster designs-, but such an approach would likely not be feasible due to time and cost restrictions. The use of multiple cameras per sampling point increases the likelihood that at least one of them is situated in a site that is used by the species (Hofmeester et al., 2021). This is especially convenient in occupancy studies targeted to rare and/or low-detectable species. In line with our results, previous studies have shown that placing at least two cameras per sampling point increased the accuracy and precision of occupancy estimates (Evans et al., 2019; Pease et al., 2016; Wong et al., 2019). Technical developments that increase the camera detection zone (e.g. 360° field of view) and/or a system that allows the camera to rotate on its main axis during a deployment could contribute to more representative and cost-efficient monitoring.

Both in clustered and single settings, an increase in precision was observed when increasing the number of sampling points (Figures 4 and 5). Previous studies have shown a relationship between population aggregation and precision (Palencia, Barroso, et al., 2022; Rowcliffe et al., 2008), suggesting that for a desired level of precision, the number of sampling points needed should increase with population aggregation. Our empirical data from eight different species corroborated this pattern, as we found the highest precision for the species with the lowest aggregation (i.e. wild boar—k overdispersion parameter of 4.18, Figure 5). Similarly, we obtained the lowest precision for species with high aggregation such as Iberian hare, red partridge, and badger (k overdispersion parameter lower than 0.5; Figure 5). In this respect, the high level of population aggregation reinforces the need to monitor a minimum of 30–40 sampling points for most species to obtain a coefficient of variation lower than 0.2 (Palencia, Barroso, et al., 2022).

We also observed similar precision between single and clustered designs, when deploying a given number of camera traps (not sampling points) simultaneously (and not rotating) and monitoring random or trail-based distributions (Figure 4, Appendix S1). From the practical point of view, clustered designs provide the easiest field implementation, and decrease the human power and time needed during fieldwork as a lower number of sampling points need to be visited. This could be especially relevant in areas with low human accessibility. On the other hand, we could hypothesize that the main disadvantage of clustered designs could be a higher risk of a cluster being affected by vandalism due to the proximity of cameras, but there is still no evidence in this regard. On the contrary, simulations suggested that deploying static cameras following a single design (i.e. maximizing the number of sampling points) could be preferred in comparison to clustered designs

when monitoring aggregated populations (Figure 4). When monitoring aggregated distributions, increasing the number of sampling points would be desirable to better reflect the areas without species presence, but also those with high species abundance (Figure 1). Thus, the large-scale population variability is higher and a higher number of sampling points is needed to capture this variability. On the contrary, in random and trail-based scenarios, the small-scale variability is higher relative to the large-scale variability (Figure 1), and thus clustered designs are more convenient to deal with small-scale variability (Figures 4 and 5). Concerning the field data, we observed that the precision was equivalent (ca. 0.05 difference in CVs) between deploying 45 cameras following a single design or clustering them, especially when the aggregation of the population was not very high (i.e. k overdispersion parameter >0.5, Figure 5). For example, in the red deer population, we obtained a coefficient of variation of 0.14 when monitoring 45 single sampling points, and a coefficient of variation of 0.13 when monitoring 15 clustered sampling points (Figure 5). Finally, we also observed that as the intensity of the point pattern increased, the difference in precision between single and clustered designs became smaller (Figure 5). This result reinforced the need to account for the abundance of the underlying population when defining the study design. Under high-abundance scenarios, the animals will use a higher proportion of the available space (not only high-quality habitat), and thus, the small-scale spatial variation in detection rates might be reduced. It is worth mentioning that we simulated perfect detection in the grid cell (10×10 m square), which is considerably higher than the area effectively monitored with a camera trap (Palencia, Barroso, et al., 2022). This assumption does not compromise the comparison among sampling designs (perfect detection was assumed in all of them) and allowed us to optimize computing resources when running the simulations.

We also explored which design strategy returned the most precise estimates when the number of camera trap devices is limited (as it usually is in real-world situations) by considering a scenario in which 15 camera devices were available. From the simulation results, we observed that rotating the cameras to independent sampling points (single designs) returns a strong improvement in precision for aggregated populations (reduction by 0.20 in CV, Figure 6). For the trail-based and random distributions, the three approaches returned similar precision (Figure 6). This result was expected because, in a scenario of random animal distribution, sampling design is irrelevant. However, no animal distribution is ever truly random. Animals are distributed according to e.g. habitat preferences, resource availability, and intra- and inter-species interactions. The lowest CV for red deer, red partridge, and wild boar was obtained by rotating the cameras to independent locations (Figure 6). These three species prefer not to use trails and their spatial distribution is equivalent to the simulated aggregated scenario (Figure 1). The improvement in precision when monitoring aggregated populations and rotating the cameras to independent locations was especially marked in the simulated medium- and high-abundance scenarios (Figure 6). In our study area,

red deer and wild boar were the most abundant species. Red deer was the most abundant species, with population densities close to 40 ind·km^{-2} (Acevedo et al., 2008) and it was the species for which we observed a stronger improvement in precision when rotating the cameras to independent placements (CV = 0.16), compared to keeping the camera fixed (CV = 0.25) or rotating them within the cluster (CV = 0.26). Regarding wild boar, population density estimates were not available for the target population. A population density close to 10 ind·km^{-2} was however reported for a population in a similar habitat less than 30 km away (Palencia et al., 2021). The only two species for which the rotating approach did not return the lowest CV were the Iberian hare and red fox (Figure 6). These results were expected considering that both species travel along trails and prefer areas near field edges (Adkins & Stott, 1998; Andersen et al., 2017; Dickie et al., 2017; Roedenbeck & Voser, 2008; Schai-Braun & Hackländer, 2014), leading to a situation similar to the trail-based simulated scenario. Iberian hare results showed similar precision independent of the design (fixed approach: 0.43, rotating within the cluster: 0.47, rotating to independent placements: 0.46, Figure 6, Appendix S3). For red fox, a CV of 0.34 was obtained for both rotating designs, while the CV was 0.25 in the fixed approach (Figure 6, Appendix S3). Our results also showed that rotating inside the cluster resulted in the lowest precision (average CV of 0.4). This is partially induced by the effect of the red partridge precision. Not considering the red partridge in the estimation of the average CV results in a more similar CV among designs (CV = 0.29 when rotating to independent placements, CV = 0.31 when rotating inside the cluster, and CV = 0.26 when keeping cameras fixed; Figure 6, Appendix S3), which is consistent with the simulation results. Important aspects to account for when applying rotating designs are both overall survey duration and the deployment duration. Previous research showed a stabilization of detection rates between 2 and 3 weeks (Kays et al., 2020); while detection rates were highly variable for the first days of camera deployment. On the other hand, survey lengths longer than 3/4 months could introduce variability in detection rates due to seasonal dynamics (e.g. resource availability, weather conditions, species detectability, movement patterns, etc.). Thus, a general recommendation when applying rotating designs could be to consider 3 weeks as the minimum deployment length, and 3/4 months as the maximum survey length (Kays et al., 2020), but this is likely to be species- and location-specific, which highlights the need to understand one's species of interest to optimize survey design.

5 | CONCLUSIONS

In conclusion, given a certain number of sampling points, our results support the use of static clustered designs when monitoring random and trail-based populations with a high number of cameras, due to an average relative reduction of more than 40% in CV when comparing a given number of sampling points, resulting in more precise detection rates (Figures 4 and 5). Clustered designs could be especially recommended in areas that are difficult to access. On the contrary, when few cameras are available, our results support the use of single designs and rotating the cameras to independent sampling points when monitoring aggregated populations, and also in cases where the target is to monitor a range of species showing different distribution patterns (Figure 6). Keeping the cameras fixed during the entire survey period is the most efficient procedure when monitoring species which frequently use linear features (e.g. trails) and random population distributions and returns similar precision in comparison to rotating the cameras (Figure 6). Broadly, this framework could be not only applied in the growing number of camera trap studies worldwide (Caravaggi et al., 2017; Delisle et al., 2021), but also to other survey methods (e.g., hair snares) that rely on detection data with corresponding spatial information.

CONFLICT OF INTEREST STATEMENT

The authors declare that they have no known competing financial interests or personal relationships that could have appeared to influence the work reported in this paper.

DATA AVAILABILITY STATEMENT

Data available from the Zenodo Repository https://zenodo.org/records/11161538 (Palencia, 2024).

ORCID

Pablo Palencia https://orcid.org/0000-0002-2928-4241

Tiago Marques https://orcid.org/0000-0002-2581-1972

Tim R. Hofmeester https://orcid.org/0000-0003-2101-5482

Joaquin Vicente https://orcid.org/0000-0001-8416-3672

Pelayo Acevedo https://orcid.org/0000-0002-3509-7696

REFERENCES

Acevedo, P., Ruiz-Fons, F., Vicente, J., Reyes-García, A. R., Alzaga, V., & Gortázar, C. (2008). Estimating red deer abundance in a wide range of management situations in Mediterranean habitats. *Journal of Zoology*, 276(1), 37–47. https://doi.org/10.1111/j.1469-7998.2008.00464.x

Adkins, C. A., & Stott, P. (1998). Home ranges, movements and habitat associations of red foxes *Vulpes vulpes* in suburban Toronto, Ontario, Canada. *Journal of Zoology*, 244(3), 335–346. https://doi.org/10.1111/j.1469-7998.1998.tb00038.x

Agha, M., Batter, T., Bolas, E. C., Collins, A. C., Gomes da Rocha, D., Monteza-Moreno, C. M., Preckler-Quisquater, S., & Sollmann, R. (2018). A review of wildlife camera trapping trends across Africa. *African Journal of Ecology*, 56(4), 694–701. https://doi.org/10.1111/aje.12565

Andersen, G. E., Johnson, C. N., Barmuta, L. A., & Jones, M. E. (2017). Use of anthropogenic linear features by two medium-sized carnivores in reserved and agricultural landscapes. *Scientific Reports*, 7(1), 11624. https://doi.org/10.1038/s41598-017-11454-z

Anderson, D. R. (2001). The need to get the basics right in wildlife field studies. *Wildlife Society Bulletin*, 29, 1294–1297.

Baddeley, A., & Turner, R. (2005). spatstat: An *R* package for analyzing spatial point patterns. *Journal of Statistical Software*, 12(6), 1–42. https://doi.org/10.18637/jss.v012.i06

Bivand, R., & Rundel, C. (2021). *geos: Interface to geometry engine-open source* ('GEOS').

Bolker, B. M. (2008). *Ecological models and data in R*. Princeton University Press.

Buckland, S. T., Anderson, D. R., Burnham, K. P., Laake, J. L., Borchers, D. L., & Thomas, L. (2001). *Introduction to distance sampling: Estimating abundance of biological populations*.

Caravaggi, A., Banks, P. B., Burton, A. C., Finlay, C. M. V., Haswell, P. M., Hayward, M. W., Rowcliffe, M. J., & Wood, M. D. (2017). A review of camera trapping for conservation behaviour research. *Remote Sensing in Ecology and Conservation*, 3(3), 109–122. https://doi.org/10.1002/rse2.48

Carbone, C., Christie, S., Conforti, K., Coulson, T., Franklin, N., Ginsberg, J. R., Griffiths, M., Holden, J., Kawanishi, K., Kinnaird, M., Laidlaw, R., Lynam, A., Macdonald, D. W., Martyr, D., McDougal, C., Nath, L., O'Brien, T., Seidensticker, J., Smith, D. J. L., … Shahruddin, W. W. (2001). The use of photographic rates to estimate densities of tigers and other cryptic mammals. *Animal Conservation*, 4, 75–79. https://doi.org/10.1017/S1367943001001081

Delignette-Muller, M. L., & Dutang, C. (2015). fitdistrplus: An *R* package for fitting distributions. *Journal of Statistical Software*, 64(4), 1–34. https://doi.org/10.18637/jss.v064.i04

Delisle, Z. J., Flaherty, E. A., Nobbe, M. R., Wzientek, C. M., & Swihart, R. K. (2021). Next-generation camera trapping: Systematic review of historic trends suggests keys to expanded research applications in ecology and conservation. *Frontiers in Ecology and Evolution*, 9, 617996. https://doi.org/10.3389/fevo.2021.617996

Dickie, M., Serrouya, R., McNay, R. S., & Boutin, S. (2017). Faster and farther: Wolf movement on linear features and implications for hunting behaviour. *Journal of Applied Ecology*, 54(1), 253–263. https://doi.org/10.1111/1365-2664.12732

Dowle, M., & Srinivasan, A. (2021). *data.table: Extension of 'data.frame'*.

du Preez, B. D., Loveridge, A. J., & Macdonald, D. W. (2014). To bait or not to bait: A comparison of camera-trapping methods for estimating leopard *Panthera pardus* density. *Biological Conservation*, 176, 153–161. https://doi.org/10.1016/j.biocon.2014.05.021

ENETWILD-consortium, Guerrasio, T., Pelayo Acevedo, P., Apollonio, M., Arnon, A., Barroqueiro, C., Belova, O., Berdión, O., Blanco-Aguiar, J. A., Bijl, H., Bleier, N., Bučko, J., Elena Bužan, E., Carniato, D., Carro, F., Casaer, J., Carvalho, J., Csányi, S., Lucía del Rio, L., … Vicente, J. (2023). Wild ungulate density data generated by camera trapping in 37 European areas: First output of the European Observatory of Wildlife (EOW). *EFSA Supporting Publications*, 20(3), 7892E.

Evans, B. E., Mosby, C. E., & Mortelliti, A. (2019). Assessing arrays of multiple trail cameras to detect North American mammals. *PLoS One*, 14(6), e0217543. https://doi.org/10.1371/journal.pone.0217543

Forrester, T., O'Brien, T., Fegraus, E., Jansen, P., Palmer, J., Kays, R., Ahumada, J., Stern, B., & McShea, W. (2016). An open standard for camera trap data. *Biodiversity Data Journal*, 4, e10197. https://doi.org/10.3897/BDJ.4.e10197

Fuller, A. K., Augustine, B. C., Morin, D. J., Pigeon, K., Boulanger, J., Lee, D. C., Bisi, F., & Garshelis, D. L. (2022). The occupancy-abundance relationship and sampling designs using occupancy to monitor populations of Asian bears. *Global Ecology and Conservation*, 35, e02075. https://doi.org/10.1016/j.gecco.2022.e02075

Garrote, G., Pérez de Ayala, R., Álvarez, A., Martín, J. M., Ruiz, M., de Lillo, S., & Simón, M. A. (2021). Improving the random encounter model method to estimate carnivore densities using data generated by conventional camera-trap design. *Oryx*, 55(1), 99–104. https://doi.org/10.1017/s0030605318001618

Green, A. M., Chynoweth, M. W., & Şekercioğlu, Ç. H. (2020). Spatially explicit capture-recapture through camera trapping: A review of benchmark analyses for wildlife density estimation. *Frontiers in Ecology and Evolution*, 8, 563477. https://doi.org/10.3389/fevo.2020.563477

Guillera-Arroita, G., & Lahoz-Monfort, J. J. (2012). Designing studies to detect differences in species occupancy: Power analysis under imperfect detection. *Methods in Ecology and Evolution*, 3(5), 860–869. https://doi.org/10.1111/j.2041-210X.2012.00225.x

Hamel, S., Killengreen, S. T., Henden, J. A., Eide, N. E., Roed-Eriksen, L., Ims, R. A., & Yoccoz, N. G. (2013). Towards good practice guidance in using camera-traps in ecology: Influence of sampling design on validity of ecological inferences. *Methods in Ecology and Evolution*, 4(2), 105–113. https://doi.org/10.1111/j.2041-210x.2012.00262.x

Hofmeester, T. R., Cromsigt, J. P. G. M., Odden, J., Andrén, H., Kindberg, J., & Linnell, J. D. C. (2019). Framing pictures: A conceptual framework to identify and correct for biases in detection probability of camera traps enabling multi-species comparison. *Ecology and Evolution*, 9, 2320–2336. https://doi.org/10.1002/ece3.4878

Hofmeester, T. R., Thorsen, N. H., Cromsigt, J. P. G. M., Kindberg, J., Andrén, H., Linnell, J. D. C., & Odden, J. (2021). Effects of camera-trap placement and number on detection of members of a mammalian assemblage. *Ecosphere*, 12(7), e03662. https://doi.org/10.1002/ecs2.3662

Howe, E. J., Buckland, S. T., Després-Einspenner, M.-L., & Kühl, H. S. (2017). Distance sampling with camera traps. *Methods in Ecology and Evolution*, 8(11), 1558–1565. https://doi.org/10.1111/2041-210X.12790

Jacobs, C. E., & Ausband, D. E. (2018). An evaluation of camera trap performance - what are we missing and does deployment height matter? *Remote Sensing in Ecology and Conservation*, 4, 352–360. https://doi.org/10.1002/rse2.81

Kays, R., Arbogast, B. S., Baker-Whatton, M., Beirne, C., Boone, H. M., Bowler, M., Burneo, S. F., Cove, M. V., Ding, P., Espinosa, S., Luis Sousa Gonçalves, A., Hansen, C. P., Jansen, P. A., Kolowski, J. M., Knowles, T. W., Guimarães Moreira Lima, M., Millspaugh, J., McShea, W. J., Pacifici, K., … Spironello, W. R. (2020). An empirical

evaluation of camera trap study design: How many, how long, and when? *Methods in Ecology and Evolution*, 11, 700–713. https://doi.org/10.1111/2041-210X.13370

Kays, R., Hody, A., Jachowski, D. S., & Parsons, A. W. (2021). Empirical evaluation of the spatial scale and detection process of camera trap surveys. *Movement Ecology*, 9(1), 41. https://doi.org/10.1186/s40462-021-00277-3

Kays, R., Tilak, S., Kranstauber, B., Jansen, P. A., Carbone, C., Rowcliffe, M. J., Fountain, T., Eggert, J., & He, Z. (2010). *Monitoring wild animal communities with arrays of motion sensitive camera traps*. http://dblp.uni-trier.de/db/journals/corr/corr1009.html#abs-1009-5718

Kolowski, J. M., & Forrester, T. D. (2017). Camera trap placement and the potential for bias due to trails and other features. *PLoS One*, 12(10), e0186679. https://doi.org/10.1371/journal.pone.0186679

Kolowski, J. M., Oley, J., & McShea, W. J. (2021). High-density camera trap grid reveals lack of consistency in detection and capture rates across space and time. *Ecosphere*, 12(2), e03350. https://doi.org/10.1002/ecs2.3350

MacKenzie, D. I., Nichols, J. D., Lachman, G. B., Droege, S., Andrew Royle, J., & Langtimm, C. A. (2002). Estimating site occupancy rates when detection probabilities are less than one. *Ecology*, 83(8), 2248–2255. https://doi.org/10.1890/02-3090

Moeller, A. K., Lukacs, P. M., & Horne, J. S. (2018). Three novel methods to estimate abundance of unmarked animals using remote cameras. *Ecosphere*, 9(8), e02331. https://doi.org/10.1002/ecs2.2331

Nakashima, Y., Fukasawa, K., & Samejima, H. (2018). Estimating animal density without individual recognition using information derivable exclusively from camera traps. *Journal of Applied Ecology*, 55(2), 735–744. https://doi.org/10.1111/1365-2664.13059

Palencia, P. (2024). Data availability: Clustered and rotating designs as a strategy to obtain precise detection rates in camera trapping studies. *Zenodo Repository*. https://doi.org/10.5281/zenodo.11161538

Palencia, P., Barroso, P., Vicente, J., Hofmeester, T. R., Ferreres, J., & Acevedo, P. (2022). Random encounter model is a reliable method for estimating population density of multiple species using camera traps. *Remote Sensing in Ecology and Conservation*, 8(5), 670–682. https://doi.org/10.1002/rse2.269

Palencia, P., Rowcliffe, J. M., Vicente, J., & Acevedo, P. (2021). Assessing the camera trap methodologies used to estimate density of unmarked populations. *Journal of Applied Ecology*, 58(8), 1583–1592. https://doi.org/10.1111/1365-2664.13913

Palencia, P., Vicente, J., Soriguer, R. C., & Acevedo, P. (2022). Towards a best-practices guide for camera trapping: Assessing differences among camera trap models and settings under field conditions. *Journal of Zoology*, 316(3), 197–208. https://doi.org/10.1111/jzo.12945

Palmer, M. S., Swanson, A., Kosmala, M., Arnold, T., & Packer, C. (2018). Evaluating relative abundance indices for terrestrial herbivores from large-scale camera trap surveys. *African Journal of Ecology*, 56(4), 791–803. https://doi.org/10.1111/aje.12566

Pease, B. S., Nielsen, C. K., & Holzmueller, E. J. (2016). Single-camera trap survey designs miss detections: Impacts on estimates of occupancy and community metrics. *PLoS One*, 11(11), e0166689. https://doi.org/10.1371/journal.pone.0166689

Pebesma, E. J., & Bivand, R. S. (2005). *Classes and methods for spatial data in R.*

R Core Team. (2022). *R: A language and environment for statistical computing*. R Foundation for Statistical Computing. https://www.R-project.org/.

Rich, L. N., Miller, D. A. W., Muñoz, D. J., Robinson, H. S., McNutt, J. W., & Kelly, M. J. (2019). Sampling design and analytical advances allow for simultaneous density estimation of seven sympatric carnivore species from camera trap data. *Biological Conservation*, 233, 12–20. https://doi.org/10.1016/j.biocon.2019.02.018

Robert, J. H. (2023). *raster: Geographic data analysis and modeling*. R package version 3.6-14 (version 3.6-14).

Roedenbeck, I. A., & Voser, P. (2008). Effects of roads on spatial distribution, abundance and mortality of brown hare (*Lepus europaeus*) in Switzerland. *European Journal of Wildlife Research*, 54(3), 425–437. https://doi.org/10.1007/s10344-007-0166-3

Rovero, F., & Zimmermann, F. (2016). *Camera Trapping for Wildlife Research (Pelagic Pu)*. Pelagic Publishing.

Rowcliffe, J. M., Field, J., Turvey, S. T., & Carbone, C. (2008). Estimating animal density using camera traps without the need for individual recognition. *Journal of Applied Ecology*, 45(4), 1228–1236. https://doi.org/10.1111/j.1365-2664.2008.01473.x

Schai-Braun, S. C., & Hackländer, K. (2014). Home range use by the European hare (*Lepus europaeus*) in a structurally diverse agricultural landscape analysed at a fine temporal scale. *Acta Theriologica*, 59(2), 277–287. https://doi.org/10.1007/s13364-013-0162-9

Scotson, L., Johnston, L. R., Iannarilli, F., Wearn, O. R., Mohd-Azlan, J., Wong, W. M., Gray, T. N. E., Dinata, Y., Suzuki, A., Willard, C. E., Frechette, J., Loken, B., Steinmetz, R., Moßbrucker, A. M., Clements, G. R., & Fieberg, J. (2017). Best practices and software for the management and sharing of camera trap data for small and large scales studies. *Remote Sensing in Ecology and Conservation*, 3(3), 158–172. https://doi.org/10.1002/rse2.54

Si, X., Kays, R., & Ding, P. (2014). How long is enough to detect terrestrial animals? Estimating the minimum trapping effort on camera traps. *PeerJ*, 2, e374. https://doi.org/10.7717/peerj.374

Sollmann, R., Mohamed, A., Samejima, H., & Wilting, A. (2013). Risky business or simple solution – Relative abundance indices from camera-trapping. *Biological Conservation*, 159, 405–412. https://doi.org/10.1016/j.biocon.2012.12.025

Stewart, F. E. C., Volpe, J. P., & Fisher, J. T. (2019). The debate about bait: A red herring in wildlife research. *The Journal of Wildlife Management*, 83(4), 985–992. https://doi.org/10.1002/jwmg.21657

Tourani, M., Brøste, E. N., Bakken, S., Odden, J., & Bischof, R. (2020). Sooner, closer, or longer: Detectability of mesocarnivores at camera traps. *Journal of Zoology*, 312(4), 259–270. https://doi.org/10.1111/jzo.12828

Vélez, J., McShea, W., Shamon, H., Castiblanco-Camacho, P. J., Tabak, M. A., Chalmers, C., Fergus, P., & Fieberg, J. (2022). An evaluation of platforms for processing camera-trap data using artificial intelligence. *Methods in Ecology and Evolution*, 14, 459–477. https://doi.org/10.1111/2041-210X.14044

Wickham, H., François, R., Henry, L., Müller, K., & Vaughan, D. (2023). *dplyr: A grammar of data manipulation*.

Wong, S. T., Belant, J. L., Sollmann, R., Mohamed, A., Niedballa, J., Mathai, J., Street, G. M., & Wilting, A. (2019). Influence of body mass, sociality, and movement behavior on improved detection probabilities when using a second camera trap. *Global Ecology and Conservation*, 20, e00791. https://doi.org/10.1016/j.gecco.2019.e00791

SUPPORTING INFORMATION

Additional supporting information can be found online in the Supporting Information section at the end of this article.

Appendix S1. Trail-based simulations in which 50% of the points were distributed across lines.

Appendix S2. R code to replicate the simulation.

Appendix S3. Coefficients of variation results.